

Optimization of Reduced-Dose MDCT of Thoracic Aorta Using Iterative Reconstruction

Hüseyin Gürkan Töre, MD, Pegah Entezari, MD, Hamid Chalian, MD,
Fernanda Dias Gonzalez-Guindalini, MD, Marcos Paulo Ferreira Botelho, MD
and Vahid Yaghmai, MD

Objective: To evaluate the contribution of iterative reconstruction on image quality of reduced-dose multidetector computed tomography of the thoracic aorta.

Methods: A torso phantom was scanned using two tube potentials (80 and 120 kVp) and five different tube currents (110, 75, 40, 20, and 10 mAs). All images were reconstructed with both filtered back projection (FBP) and iterative reconstruction. Aortic attenuation, image noise within the thoracic aorta, signal-to-noise ratio, and sharpness of the aortic wall were quantified in the phantom for the two reconstruction algorithms. Data were analyzed using paired *t* test. A value of $P < 0.05$ was considered significant.

Results: The aortic attenuation was similar for FBP and iterative reconstruction ($P > 0.05$). Image noise level was lower ($P < 0.0001$), and image sharpness was higher ($P = 0.046$) with iterative reconstruction. Signal-to-noise ratios were higher with iterative reconstruction compared with those with FBP ($P < 0.0001$). Signal-to-noise ratio at 80 kVp with iterative reconstruction (9.8 ± 4.4) was similar to the signal-to-noise ratio at 120 kVp with FBP (8.4 ± 3.3) ($P = 0.196$).

Conclusions: Less image noise and higher image sharpness may be achieved with iterative reconstruction in reduced-dose multidetector computed tomography of the thoracic aorta.

Key Words: aorta, MDCT angiography, iterative reconstruction, filtered back projection, image quality, radiation dose reduction

(*J Comput Assist Tomogr* 2014;38: 72–76)

Since its introduction in the 1970s, computed tomographic (CT) technology has undergone dramatic advances that have revolutionized patient care and increased diagnostic accuracy in a wide range of clinical indications. These developments have led to an increase in the number of CT examinations, which in turn have raised concerns about radiation dose and patient safety.^{1,2}

Computed tomographic angiography (CTA) of the thoracic aorta is routinely performed with or without electrocardiography (ECG) gating to evaluate aneurysms, dissections, and integrity of endovascular repairs. Several strategies have resulted in a reduction of radiation dose in CTA of the aorta. These include tube current modulation, tube voltage reduction, and application of body mass index–based protocols.³ The use of prospective ECG triggering is another technique that can further improve image quality and help reduce radiation dose because it can result in 53.7 and 44.2% reduction in dose with 100 and 120 kVp, respectively, using similar tube current settings when compared

with retrospective ECG-gated helical scanning.⁴ Radiation dose from thoracic aorta CTA has been reported to be 2.9 and 26.2 mSv for prospectively and retrospectively gated CTA of the aorta, respectively.⁵

Computed tomography radiation dose reduction can be achieved to a certain degree with these acquisition techniques but at the cost of increased image noise using the current filtered back projection (FBP) algorithms.⁶ Recently, iterative reconstruction has become available in clinical settings as a novel method to reduce CT image noise when radiation dose has been reduced.

In the FBP technique, projections or views are constructed from the raw data. These projections are first filtered then back projected to form a 2-dimensional array of voxels that are allotted to a gray tone that is proportional to the average x-ray photon distribution of each voxel.⁷ On the other hand, iterative reconstruction methods consist of 3 major steps. First, artificial raw data are created by a forward projection of the volumetric object estimate. This artificial raw data, in a second step, are compared with the real measured raw data to compute a correction term. In the last step, the correction term is back projected onto the volumetric object estimate. The iteration process can be initiated with an empty image estimate or using prior information.⁸ An example of an iterative reconstruction that uses the image or slice data alone is iterative reconstruction in image space (IRIS). With this technique, the raw data are first reconstructed in the traditional fashion with the use of the FBP. This information is then forward projected with multiple iterations according to modeling of the noise data.⁷

Although iterative reconstruction does not affect radiation dose directly, it might lead to less radiation exposure in CT imaging by maintaining diagnostic image quality despite low radiation dose image acquisitions.⁹

The purpose of our study was to evaluate the image quality in multidetector computed tomography (MDCT) of thoracic aorta images acquired with standard and low-dose techniques and reconstructed with FBP and iterative reconstruction in an adult-sized anthropomorphic phantom.

MATERIALS AND METHODS

Image Acquisition

A custom anthropomorphic torso phantom was used to evaluate image quality of CT scans with varying tube voltages and tube currents (Fig. 1). The phantom was scanned with tube potentials of 80 and 120 kVp at the same session. At each tube potential, we performed 5 acquisitions with fixed tube current settings of 10, 20, 40, 75, and 110 mAs (10 acquisitions in total). All images were reconstructed with both filtered back projection and iterative reconstruction algorithms. A total of 20 data sets were obtained. The CT attenuation coefficients of anatomic structures in this phantom are similar to those of previous studies with attenuation of aorta measuring 190 Hounsfield units (HU) at

From the Department of Radiology, Northwestern Memorial Hospital, Northwestern University-Feinberg School of Medicine, Chicago, IL.

Received for publication January 24, 2013; accepted June 24, 2013.

Reprints: Vahid Yaghmai, MD, Department of Radiology, Northwestern Memorial Hospital, Northwestern University-Feinberg School of Medicine, 676 North Saint Clair St, Suite 800, Chicago, IL 60611 (e-mail: v-yaghmai@northwestern.edu).

Hüseyin Gürkan Töre, Pegah Entezari, Hamid Chalian, Fernanda Dias Gonzalez-Guindalini, and Marcos Paulo Ferreira Botelho are supported by an educational grant from Siemens Healthcare.

Copyright © 2014 by Lippincott Williams & Wilkins

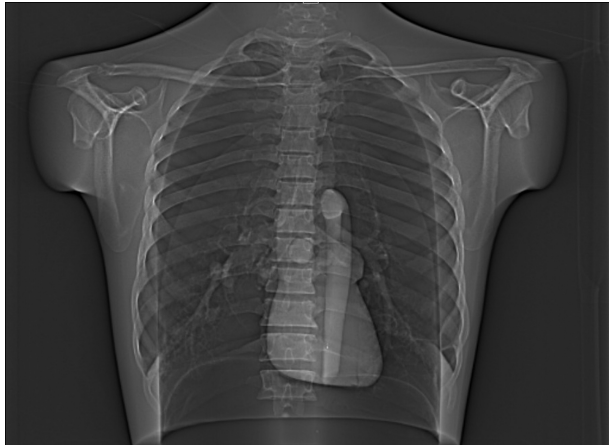


FIGURE 1. Tomogram of the adult anthropomorphic torso phantom.

120 kVp.¹⁰ Phantom was scanned with Siemens Somatom Definition AS 64-detector CT scanner (Siemens Medical Solutions, Erlangen, Germany). Data sets were acquired using a helical scan with 3-mm slice thickness and 1.5 mm of slice intervals, detector collimation of 64 × 0.6 mm, pitch of 0.8, and a gantry rotation time of 0.5 seconds. The reconstruction kernels were B40f for FBP and I40f for IRIS.

The scan length was identical for all acquisitions. Image quality was evaluated quantitatively (described in detail in the Image Analysis section). Computed Tomography Dose Index-volume and Dose Length Product were recorded for each acquisition. Effective dose was calculated using the following formula: Effective Dose = DLP × k [k = 0.014 mSv/(mGy × cm)].¹¹

Image Analysis

For each data set, aortic attenuation, image noise, and image sharpness were measured. Mean aortic attenuation in HU was measured 3 times within the descending aorta at the level of the carina using circular regions of interest. The SD of each of these measurements was recorded as *image noise*. The mean of these measures was calculated as the mean aortic attenuation and mean image noise, respectively. The signal-to-noise ratio (SNR) was calculated by dividing the mean aortic attenuation value by the image noise.

Image Sharpness

Spatial resolution in CT, as a function of blurriness, is calculated by modulation transfer function as line pairs per 1 cm. To obtain the modulation transfer function, first, the line-spread function is calculated using a fine wire or narrow slits in dedicated image quality phantoms. Then, the modulation transfer function is mathematically derived from the line-spread function.¹² In our phantom, we calculated image sharpness by plotting the attenuation difference over distance between the simulated thoracic aorta and surrounding tissue interface and calculating the slope of the resultant curve. A similar approach to quantify image sharpness has been described in more complex methods for novel segmentation algorithms.¹³ This quantifiable method may be applied for evaluation of image quality in CT images obtained for routine clinical practice.

Image sharpness was evaluated using Java-based image processing software available from the National Institutes of Health (Rasband WS. ImageJ, U. S. National Institutes of Health, Bethesda, Maryland, USA, <http://imagej.nih.gov/ij/>, 1997–2012.).¹⁴ The DICOM image of the selected slice at the level of the carina was uploaded to ImageJ. Then, using a line tool with 3 pixel thickness, a straight line was drawn across the aorta medio-laterally, allowing the line to extend 5 mm distal to the aorta wall on each side. Attenuation values within this range were plotted against the distance (Fig. 2). The mean slope of the plots on each side was calculated to obtain image sharpness. A higher slope represents higher image sharpness.¹⁵

Statistical Analysis

All analyses were performed using MedCalc version 12.2 software. Kolmogorov-Smirnov test was used to detect a normal Gaussian distribution. Normally distributed continuous variables were presented as mean ± SD (95% confidence interval). Aortic attenuation, image noise, SNR, and image sharpness for IRIS and FBP were compared using paired *t* test. A value of *P* < 0.05 was considered significant.

RESULTS

Aortic attenuation, image noise, SNR, and image sharpness for each tube voltage and tube current settings with FBP and IRIS as well as radiation dose at these settings are summarized in Table 1.

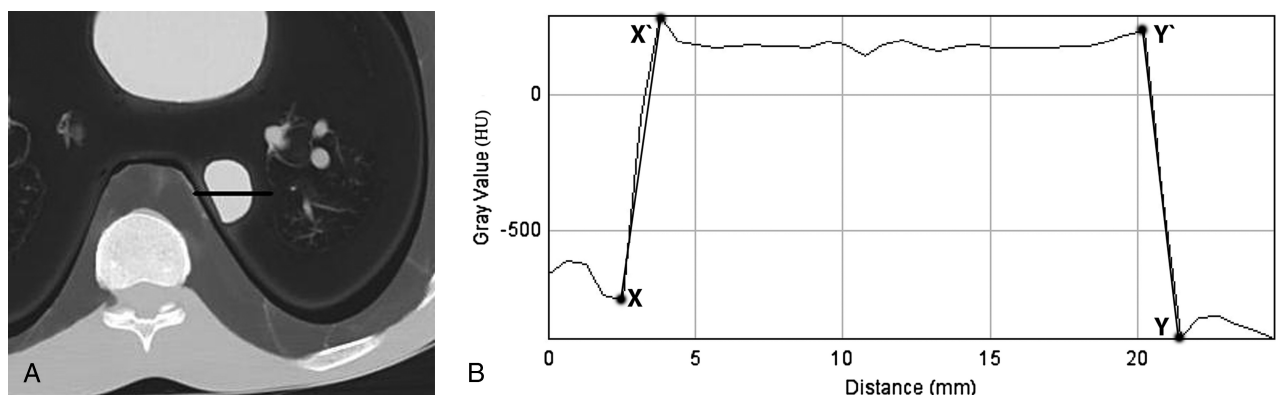


FIGURE 2. Measurement of image sharpness. A line was drawn across the aorta lumen (A), and CT attenuation values were plotted for each point along the line (B). The highest and lowest attenuation values on each side of the thoracic aorta are demonstrated as X-X' on the left and Y-Y' on the right. Slopes of the lines drawn between X-X' and Y-Y' are calculated, and their mean is recorded as the image sharpness of each acquisition.

TABLE 1. Aorta Image Quality and Radiation Dose of Each Acquisition Setting in CTA of Anthropomorphic Torso Phantom

Protocol		Aorta Attenuation, HU		Image Noise (SD)		SNR		Image Sharpness		Radiation Dose	
kVp	mAs	FBP	IRIS	FBP	IRIS	FBP	IRIS	FBP	IRIS	CTDI _{vol} , mGy	Effective Dose, mSv
80	10	279.8	274.1	88.5	59.5	3.2	4.6	0.37	1.27	0.21	0.09
80	20	273.1	281.5	63.0	43.1	4.3	6.5	0.85	1.30	0.42	0.21
80	40	278.7	280.0	45.5	29.2	6.1	9.6	1.04	1.36	0.81	0.40
80	75	279.4	277.7	34.2	19.1	8.2	14.5	1.18	1.36	1.56	0.77
80	110	278.2	279.8	24.1	20.2	11.5	13.8	1.25	1.37	2.28	1.13
120	10	188.7	189.9	47.2	27.0	4.0	7.0	1.24	1.27	0.76	0.37
120	20	187.8	187.3	26.6	15.9	7.1	11.8	1.27	1.31	1.52	0.74
120	40	193.1	192.6	23.8	14.4	8.1	13.4	1.35	1.36	3.04	1.49
120	75	191.4	191.2	19.3	12.9	9.9	14.8	1.39	1.41	5.67	2.78
120	110	189.7	189.7	14.5	9.3	13.1	20.4	1.43	1.44	8.28	4.13
<i>P</i>		>0.05		<0.0001		<0.0001		<0.05			

Aortic Attenuation

When data from both FBP and IRIS settings were taken into account, mean aortic attenuation was significantly higher at 80 kVp settings compared with that at 120 kVp settings, which were 278.2 ± 2.6 HU and 190.1 ± 1.9 HU, respectively ($P < 0.0001$).

When compared cumulatively at all tube voltages, aortic attenuations were similar for both FBP (233.9 ± 46.2 HU) and IRIS (234.3 ± 46.6 HU) ($P > 0.05$). When compared separately, aortic attenuations for both FBP and IRIS were similar at 80 kVp ($P = 0.7531$) and at 120 kVp ($P = 0.9875$).

Image Noise and SNR

There was an increase in image noise with a decreasing tube current (Fig. 3). Image noise for both tube voltages was lower with IRIS compared with FBP ($P < 0.0001$). Image noise at 80 kVp was 51.06 ± 25.42 HU and 34.22 ± 17.09 HU, for FBP and IRIS, respectively ($P = 0.0142$) (Fig. 3). Image noise at 120 kVp was 26.28 ± 12.56 HU and 15.90 ± 6.67 HU for FBP and IRIS, respectively ($P = 0.0172$).

Signal-to-noise ratios for both tube voltages were higher with IRIS (11.6 ± 4.7) compared with those with FBP (7.55 ± 3.28) ($P < 0.0001$). The SNR at 80 kVp with IRIS was similar to the SNR at 120 kVp with FBP ($P = 0.196$).

Image Sharpness

Images reconstructed with IRIS were sharper than images reconstructed with FBP ($P = 0.046$) (Fig. 4A, B). At 80 kVp, the mean image sharpness values for FBP and IRIS were 0.93 ± 0.35 HU and 1.33 ± 0.04 HU, respectively ($P = 0.04$). Mean image sharpness values at 120 kVp for FBP and IRIS were 1.33 ± 0.08 and 1.35 ± 0.06 HU, respectively ($P = 0.04$).

Image Quality and Radiation Dose

Effective radiation doses increased with higher tube currents applied at both 80 and 120 kVp (Fig. 5). The lowest image noise with FBP was 14.5 when imaged at 120 kVp/110 mAs setting (SNR = 13.1). A similar image noise level (14.4) was obtained at a lower mAs setting, with IRIS at 120 kVp/40 mAs setting (SNR = 13.4). Effective radiation dose levels were 4.13 and 1.49 mSv for 120 kVp/110 mAs and 120 kVp/40 mAs settings, respectively.

Similar noise levels were observed at 120 kVp/75 mAs setting with FBP (19.3) and 80 kVp/75 mAs setting with IRIS (19.1) (SNR = 9.9 and SNR = 14.5, respectively). Effective dose levels were 2.78 and 0.77 mSv for 120 kVp/75 mAs setting with FBP and 80 kVp/75 mAs setting with IRIS, respectively.

DISCUSSION

In the conventional FBP algorithm, a projection of the acquired raw data is formed and an initial image is produced by back projecting these new data. However, a so-called starlike blurring artifact occurs by this process and a filter is applied to eliminate this artifact.⁷ In IRIS, on the other hand, the reconstruction process is on the forward direction.⁸ Improvement of the image noise is maintained by correction loops that compares acquired data with the estimated data. Although iterative reconstruction was introduced in the early CT prototypes, it has not been generally applied in routine imaging until recently because of high computational power requirements. The development of new graphic processor units has made iterative reconstruction clinically available, whereas the reconstruction time for IRIS is only slightly longer than that for the FBP.^{7,16} Compared with the current filtered back projection reconstruction algorithm,

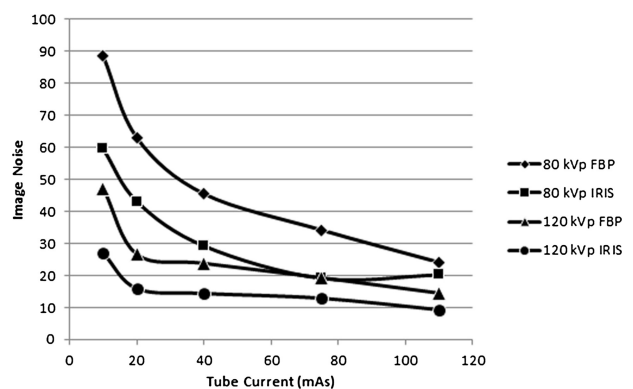


FIGURE 3. Plots of image noise versus different tube currents comparing 80 kVp with 120 kVp with and without IRIS. Diamonds represent image noise with 80 kVp-FBP, squares represent image noise with 80 kVp-IRIS, triangles represent image noise with 120 kVp-FBP, and circles represent image noise with 120 kVp-IRIS settings. Note different scales of image noise for FBP and IRIS.

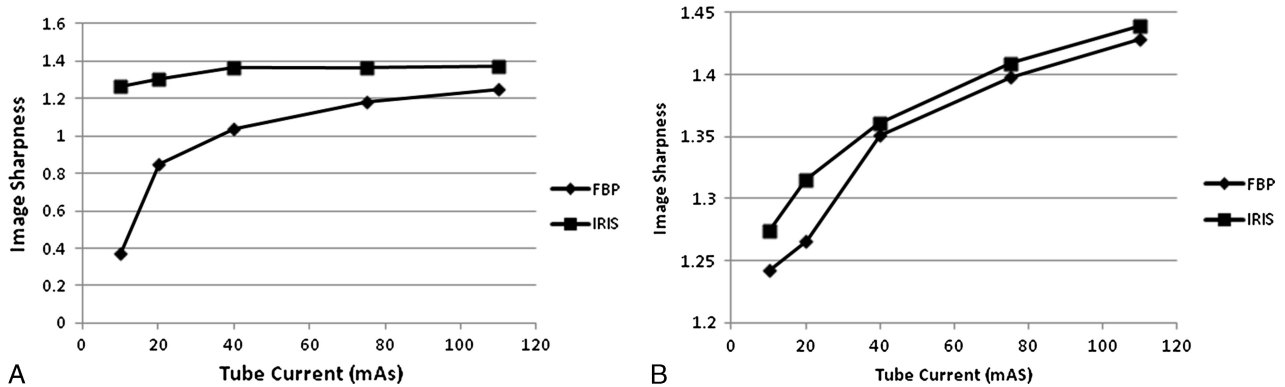


FIGURE 4. Plots of image sharpness versus different tube currents comparing FBP with IRIS for 80 kVp and 120 kVp. A, Tube voltage of 80 kVp. B, Tube voltage of 120 kVp. Diamonds represent image noise with FBP, and squares represent image noise with IRIS. Please note that the difference in image sharpness is accentuated as tube current decreases.

this new technique may improve image quality with a reduced image noise.⁹

In this study, we investigated the effect of iterative reconstruction with different tube voltage and current settings on image quality of thoracic aorta CTA. Results of this study demonstrate no significant difference in the aortic attenuation comparing different reconstruction algorithms. On the other hand, similar to previous studies, changing tube voltage affected aortic attenuation measurements.¹⁷ Lowering tube voltage results in higher attenuation measurements because the photon energy at 80 kVp is closer to the K_{edge} of iodine.¹⁸

In our study, lowering tube voltage and/or tube current resulted in an increase in image noise. However, with the iterative reconstruction technique, the image noise was significantly lower than with the FBP technique in the same acquisition settings. There was an increase in image noise with FBP as tube current decreased, whereas an increase in image noise was compensated with IRIS. These results suggest that, compared with FBP, more acceptable image quality may be obtained with the iterative reconstruction technique when images are acquired with very low dose settings. Correspondingly, SNR was higher with iterative reconstruction. Signal-to-noise ratios at 80 kVp with IRIS were comparable to SNRs at 120 kVp with FBP. Considering these parameters as an objective method of image quality assessment, these results suggest that background noise was better compensated for by iterative reconstruction.

This study allows comparison of image quality and radiation exposure at different acquisition settings. Acquisition settings with the lowest image noise at 120 kVp/110 mAs revealed an image noise of 14.5 when FBP was used. Effective dose at this setting was 4.13 mSv. Comparable image noise of 14.4 was obtained with 120 kVp/40 mAs settings with iterative reconstruction. Despite the similar image noise, effective dose was 1.49 mSv at this setting. Even with a very low dose of 0.77 mSv at 80 kVp/75 mAs with iterative reconstruction, only a slightly higher image noise of 19.1 was observed. Our results suggest that low-dose CTA of the aorta can be performed at approximately 50% of the standard dose without affecting image noise and with increasing aortic attenuation when iterative reconstruction is used.

In a qualitative analysis by Winklehner et al,¹⁹ a better image sharpness was obtained with iterative reconstruction. Our results are consistent with those of their study in achieving higher quantitative image sharpness with iterative reconstruction in all tube voltage and tube current settings. Although the difference in image sharpness with FBP and IRIS was smaller in higher

radiation dose settings, this difference was more apparent at lower tube currents. It was also notable that the difference in image sharpness between FBP and IRIS algorithms was more prominent at 80 kVp.

Our study had limitations. In this phantom study, we evaluated only 2 kVp settings; the effect of kVp settings less than 80 kVp and more than 120 kVp may be of interest in pediatric and large adult patients, respectively. If the same trends of results on this study occur, it is expected that the use of iterative reconstruction may lead to lower image noise and higher SNR levels at any voltage when compared with FBP values for the same acquisition parameters. However, future studies assessing different kVp settings are warranted. Because it is not feasible to rescan human subjects with varying radiation dose settings in the same setting, we could not test our results in the clinical environment. As diagnostic confidence requirements for different pathologies of the thoracic aorta may vary, further studies to evaluate diagnostic quality of CT image acquisitions with other combinations of tube parameter adjustments are warranted. In addition, motion artifacts, such as breathing, were not evaluated in this phantom study. The possibility of these artifacts should be taken into consideration in future clinical studies. Furthermore, our study was focused on evaluation of different tube voltage and tube current settings with and without iterative reconstruction on high-contrast structures, such as the thoracic aorta. Studies evaluating the effects of these parameters on low-contrast structures are warranted.

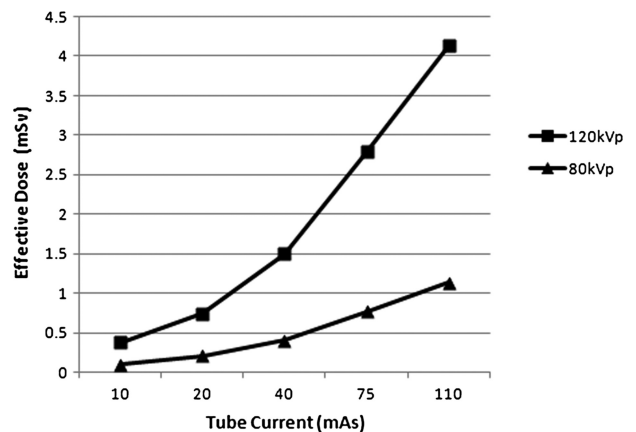


FIGURE 5. Plots of effective dose versus tube current for 80 kVp and 120 kVp. Triangles represent dose at 80 kVp, and squares represent dose at 120 kVp.

In conclusion, lower radiation exposure with better image quality in MDCT of the thoracic aorta is possible with the application of iterative reconstruction.

REFERENCES

1. Pauwels EK, Bourguignon M. Cancer induction caused by radiation due to computed tomography: a critical note. *Acta Radiol.* 2011;52:767–773.
2. Huda W. Radiation doses and risks in chest computed tomography examinations. *Proc Am Thorac Soc.* 2007;4:316–320.
3. Coakley FV, Gould R, Yeh BM, et al. CT radiation dose: what can you do right now in your practice? *AJR Am J Roentgenol.* 2011;196:619–625.
4. Blanke P, Bulla S, Baumann T, et al. Thoracic aorta: prospective electrocardiographically triggered CT angiography with dual-source CT—feasibility, image quality, and dose reduction. *Radiology.* 2010;255:207–217.
5. Farrelly C, Davarpanah A, Keeling AN, et al. Low-dose dual-source CT angiography of the thoracic aorta. *Int J Cardiovasc Imaging.* 2011;27:1025–1034.
6. Alkadhi H, Schindera ST. State of the art low-dose CT angiography of the body. *Eur J Radiol.* 2011;80:36–40.
7. Nelson RC, Feuerlein S, Boll DT. New iterative reconstruction techniques for cardiovascular computed tomography: how do they work, and what are the advantages and disadvantages? *J Cardiovasc Comput Tomogr.* 2011;5:286–292.
8. Beister M, Kolditz D, Kalender WA. Iterative reconstruction methods in X-ray CT. *Phys Med.* 2012;28:94–108.
9. Hu XH, Ding XF, Wu RZ, et al. Radiation dose of non-enhanced chest CT can be reduced 40% by using iterative reconstruction in image space. *Clin Radiol.* 2011;66:1023–1029.
10. Birnbaum BA, Hindman N, Lee J, et al. Multi-detector row CT attenuation measurements: assessment of intra- and interscanner variability with an anthropomorphic body CT phantom. *Radiology.* 2007;242:109–119.
11. Christner JA, Kofler JM, McCollough CH. Estimating effective dose for CT using dose-length product compared with using organ doses: consequences of adopting International Commission on Radiological Protection publication 103 or dual-energy scanning. *AJR Am J Roentgenol.* 2010;194:881–889.
12. Watanabe H, Honda E, Kurabayashi T. Modulation transfer function evaluation of cone beam computed tomography for dental use with the oversampling method. *Dentomaxillofac Radiol.* 2010;39:28–32.
13. Xu J, Napel S, Greenspan H, et al. Quantifying the margin sharpness of lesions on radiological images for content-based image retrieval. *Med Phys.* 2012;39:5405–5418.
14. Rasband WS. ImageJ, U. S. National Institutes of Health, Bethesda, Maryland, USA, <http://imagej.nih.gov/ij/>, 1997–2012.
15. Groves EM, Bireley W, Dill K, et al. Quantitative analysis of ECG-gated high-resolution contrast-enhanced MR angiography of the thoracic aorta. *AJR Am J Roentgenol.* 2007;188:522–528.
16. Hara AK, Paden RG, Silva AC, et al. Iterative reconstruction technique for reducing body radiation dose at CT: feasibility study. *AJR Am J Roentgenol.* 2009;193:764–771.
17. Murazaki H, Funama Y, Sugaya Y, et al. Optimal setting of automatic exposure control based on image noise and contrast on iodine-enhanced CT. *Acad Radiol.* 2012;19:478–484.
18. Kalva SP, Sahani DV, Hahn PF, et al. Using the K-edge to improve contrast conspicuity and to lower radiation dose with a 16-MDCT: a phantom and human study. *J Comput Assist Tomogr.* 2006;30:391–397.
19. Winklehner A, Karlo C, Puippe G, et al. Raw data-based iterative reconstruction in body CTA: evaluation of radiation dose saving potential. *Eur Radiol.* 2011;21:2521–2526.